Theoretical and Applied Genetics (2020) 133:3455–3467
https://doi.org/10.1007/s00122-020-03680-3

ORIGINAL ARTICLE

Dissection and physical mapping of wheat chromosome 7B by inducing meiotic recombination with its homoeologues in *Aegilops speltoides* and *Thinopyrum elongatum*

Mingyi Zhang[1] · Wei Zhang[1] · Xianwen Zhu[1] · Qing Sun[2] · Changhui Yan[2] · Steven S. Xu[3] · Jason Fiedler[3] · Xiwen Cai[1]

Received: 31 March 2020 / Accepted: 4 September 2020 / Published online: 15 September 2020

Abstract

Key message **We constructed a homoeologous recombination-based bin map of wheat chromosome 7B, providing a unique physical framework for further study of chromosome 7B and its homoeologues in wheat and its relatives.**

Abstract Homoeologous recombination leads to the dissection and diversification of the wheat genome. Advances in genome sequencing and genotyping have dramatically improved the efficacy and throughput of homoeologous recombination-based genome studies and alien introgression in wheat and its relatives. In this study, we aimed to physically dissect and map wheat chromosome 7B by inducing meiotic recombination of chromosome 7B with its homoeologues 7E in *Thinopyrum elongatum* and 7S in *Aegilops speltoides*. The special genotypes, which were double monosomic for chromosomes 7B' + 7E' or 7B' + 7S' and homozygous for the *ph1b* mutant, were produced to enhance 7B – 7E and 7B – 7S recombination. Chromosome-specific DNA markers were developed and used to pre-screen the large recombination populations for 7B – 7E and 7B – 7S recombinants. The DNA marker-mediated preselections were verified by fluorescent genomic in situ hybridization (GISH). In total, 29 7B – 7E and 61 7B – 7S recombinants and multiple chromosome aberrations were recovered and delineated by GISH and the wheat 90 K SNP assay. Integrated GISH and SNP analysis of the recombinants physically mapped the recombination breakpoints and partitioned wheat chromosome 7B into 44 bins with 523 SNPs assigned within. A composite bin map was constructed for chromosome 7B, showing the bin size and physical distribution of SNPs. This provides a unique physical framework for further study of chromosome 7B and its homoeologues. In addition, the 7B – 7E and 7B – 7S recombinants extend the genetic variability of wheat chromosome 7B and represent useful germplasm for wheat breeding. Thereby, this genomics-enabled chromosome engineering approach facilitates wheat genome study and enriches the gene pool of wheat improvement.

Introduction

Common wheat (*Triticum aestivum* L., $2n = 6x = 42$), one of the most important food crops for humans worldwide, originated from hybridization involving three or more diploid ancestors and subsequent chromosome doubling (Feldman and Levy 2012; Faris 2014; Zhang et al. 2018a; Pont et al. 2019). The polyploid origin of the wheat genome and extensive breeding practices have narrowed down the genetic variability of the wheat genome, which has become a genetic bottleneck for modern wheat improvement (Venske et al. 2019). The wild relatives of wheat maintain considerable genetic diversity, including numerous favorable genes for agronomically important traits of wheat. Many of them contain a genome homoeologous with the wheat genome. They represent an invaluable gene source for wheat improvement

Communicated by P. Heslop-Harrison.

Electronic supplementary material The online version of this article (https://doi.org/10.1007/s00122-020-03680-3) contains supplementary material, which is available to authorized users.

✉ Xiwen Cai
xiwen.cai@ndsu.edu

[1] Department of Plant Sciences, North Dakota State University, Fargo, ND 58108, USA

[2] Department of Computer Science, North Dakota State University, Fargo, ND 58108, USA

[3] USDA-ARS, Cereal Crops Research Unit, Edward T. Schafer Agricultural Research Center, Fargo, ND 58102, USA

and can be utilized to expand genetic variability of wheat by diversifying and enriching the wheat genome (Qi et al. 2007; Zhang et al. 2017).

Meiotic homoeologous recombination-based chromosome engineering shuffles the genetic material of related genomes and leads to gene introgression from one genome to another. It has been widely used in alien introgression and genome studies of wheat and its relatives (Liu et al. 2013; Zhao et al. 2013; Niu et al. 2014; Danilova et al. 2017; Zhang et al. 2018a, b, 2019; Li et al. 2019; Dai et al. 2020). Wheat has a diploidization system, controlled by *Ph* (pairing homoeologous) genes. The *Ph* genes ensure homologous pairing and recombination by preventing homoeologous chromosomes from pairing and recombination in meiosis (Riley and Chapman 1958; Riley et al. 1959). So, eliminating or inactivating *Ph* genes enhances homoeologous pairing and recombination. Wheat *ph1b* mutant, a large deletion at the *Ph1* locus (Riley and Chapman 1958; Riley et al. 1959; Sears 1977; Gyawali et al. 2019), has been used to induce meiotic homoeologous recombination for chromosome mapping and alien introgression (Naranjo and Fernández-Rueda 1996; Lukaszewski et al. 2004; Niu et al. 2011; Zhao et al. 2013; Rey et al. 2015; Patokar et al. 2016; Danilova et al. 2017; Zhang et al. 2018b). Through this approach, wheat chromosomes 2B and 3B were partitioned and physically mapped (Zhang et al. 2018b, 2020). Two wild species-derived disease resistance genes were identified, mapped, and introgressed into wheat by homoeologous recombination (Zhang et al. 2019).

Wheat has a complex polyploid genome with three homoeologous subgenomes (A, B, and D). Homoeologous recombination-based partitioning and dissection of individual chromosomes provide a unique approach for genome study in wheat and its relatives. Wheat aneuploids and deletion stocks have been developed and employed to physically dissect the wheat genome and individual chromosomes (Sears 1954, 1966; Gill and Gill 1991; Endo and Gill 1996; Qi et al. 2003). In addition, various wheat-alien species chromosome translocations have been produced and applied in chromosome dissection and mapping (Chen et al. 1995, 2005; Friebe et al. 1996; Rabinovich 1998; Crasta et al. 2000; Zhao et al. 2013). Generally, meiotic homoeologous recombination-derived translocations or recombinants are genetically more stable than non-compensating translocations, and more useful for alien introgression in germplasm development. Also, meiotic homoeologous recombinants are invaluable resources for genome and chromosome studies, including physical mapping, gene identification, and genome evolution (Riley et al. 1968; Mago et al. 2002; Chen et al. 2005; Niu et al. 2011; Zhao et al. 2013; King et al. 2018; Zhang et al. 2018a, b, 2019; Dai et al. 2020; Zhang et al. 2020).

The reference genome sequences and high-throughput genotyping technologies have dramatically improved the efficacy and throughput of homoeologous recombination-based chromosome engineering for alien introgression and genome studies in wheat and its relatives (Wang et al. 2014; The International Wheat Genome Sequencing Consortium (IWGSC) 2018; Avni et al. 2017; Luo et al. 2017; Ling et al. 2018; Danilova et al. 2014, 2017; Zhang et al. 2017, 2018a, b, 2019; Dai et al. 2020; Wang et al. 2020). Wheat chromosomes can be painted differentially from those in the homoeologous genomes of wheat-related species by fluorescent genomic in situ hybridization (GISH), allowing for visual detection of chromosomal segments with different genomic origin in homoeologous recombinants (Schwarzacher et al. 1992; Cai et al. 1998; Zhao et al. 2013; Niu et al. 2014; Zhang et al. 2018b, 2019; Li et al. 2019; Zhang et al. 2020). Recently, the high-throughput SNP genotyping technology and SNP-derived PCR marker systems, including kompetitive allele specific PCR (KASP) (Neelam et al. 2013) and semi-thermal asymmetric reverse PCR (STARP) (Long et al. 2017; Zhang et al. 2017), have permitted the homoeologous recombination-based genome study and alien introgression in a significantly improved throughput (Danilova et al. 2017, 2019; Zhang et al. 2017, 2018a, b, 2019; Grewal et al. 2020). GISH and SNP markers demarcate wheat and alien chromosomal segments in the homoeologous recombinants at the cytological and molecular levels, respectively. Integrative GISH and marker analysis of homoeologous recombination leads to the construction of unique physical frameworks useful for genome studies in wheat and its relatives (Zhang et al. 2018b, 2020). In this study, we aimed to cytogenetically dissect wheat chromosome 7B by inducing meiotic recombination with its homoeologous counterparts 7E from *Th. elongatum* ($2n=2x=14$, EE) and 7S from *Ae. speltoides* ($2n=2x=14$, SS), and to physically map chromosome 7B by delineating the 7B-7E and 7B-7S recombinants with SNP markers and GISH.

Materials and methods

Plant materials

Common wheat 'Chinese Spring' (CS)—*Ae. speltoides*–disomic substitution line 7S(7B) [DS 7S(7B)] (Friebe et al. 2011) and CS *ph1b* mutant were supplied by the wheat Genetics Resource Center at Kansas State University, USA. The CS-*Th. elongatum* disomic substitution line 7E(7B) [DS 7E(7B)] was provided by J. Dvorak at University of California, Davis, USA.

Construction of the *ph1b*-induced homoeologous recombination populations

We constructed two special genotypes by crossing DS 7S(7B) and DS 7E(7B) to the CS *ph1b* mutant as illustrated in Fig. 1. The newly constructed genotypes were homozygous for the *ph1b* mutant and double monosomic for chromosomes 7E' + 7B' or 7S' + 7B'. The *Ph1*-specific molecular marker *PSR574* or *PSR128* (Roberts et al. 1999) was used to select the individuals homozygous *ph1b* mutant for inducing homoeologous 7E − 7B and 7S − 7B recombination. The chromosome 7E-specific marker *Xgpw1164* and 7S-specific marker *Xgpw7518* were used to select the individuals double monosomic for chromosome 7E' + 7B' and for chromosomes 7S' + 7B', respectively (Sourdille et al. 2004). Meiotic homoeologous recombination of wheat chromosome 7B with *Th. elongatum* chromosome 7E and *Ae. speltoides* chromosome 7S was induced by the *ph1b* mutant in the special genotypes. 7B − 7E and 7B − 7S recombinant gametes were recovered by backcrossing to the respective substitution line as described by Zhang et al. (2017, 2020).

Molecular markers analysis

Chromosome-specific STARP markers were developed within the pericentromeric and distal regions on both arms for the homoeologous pairs 7B-7E and 7B-7S (Long et al. 2017; Zhang et al. 2017). They were used to screen the recombination populations for 7B − 7E and 7B − 7S recombinants and chromosome aberrations involving the pericentromeric and distal regions of both homoeologous pairs as illustrated in Fig. 2. PCR was performed as described by Long et al. (2017). STARP amplicons were sorted using IR^2 4200 DNA Analyzer with denaturing polyacrylamide gel electrophoresis (LI-COR, Lincoln, NE, USA).

Wheat 90 K SNP assay was performed on the Illumina BeadStation and iScan instruments following the manufacturer's protocols. GenomeStudio v2.0.4 software was used

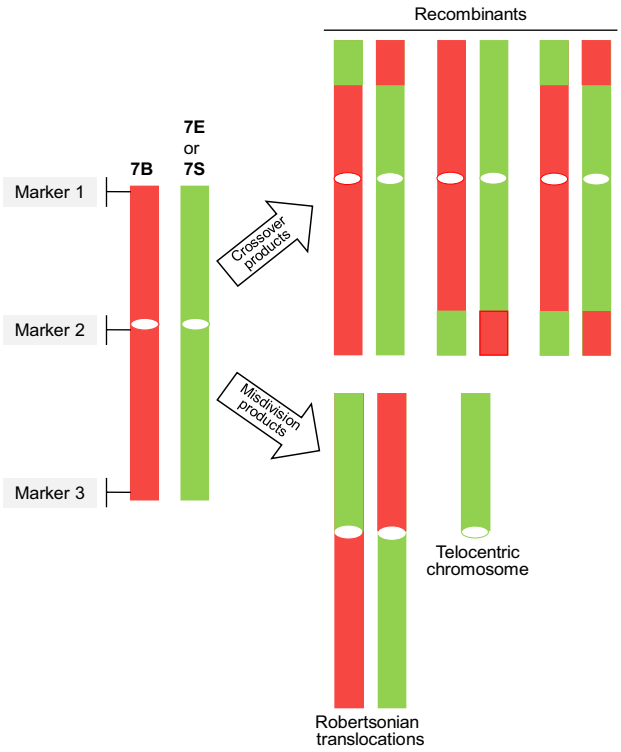

Fig. 2 Ideogram of wheat chromosome 7B (red), *Th. elongatum* chromosome 7E (green), and *Ae. speltoides* chromosome 7S (green) illustrating chromosome-specific molecular markers for the detection of meiotic homoeologous recombinants and chromosome aberrations

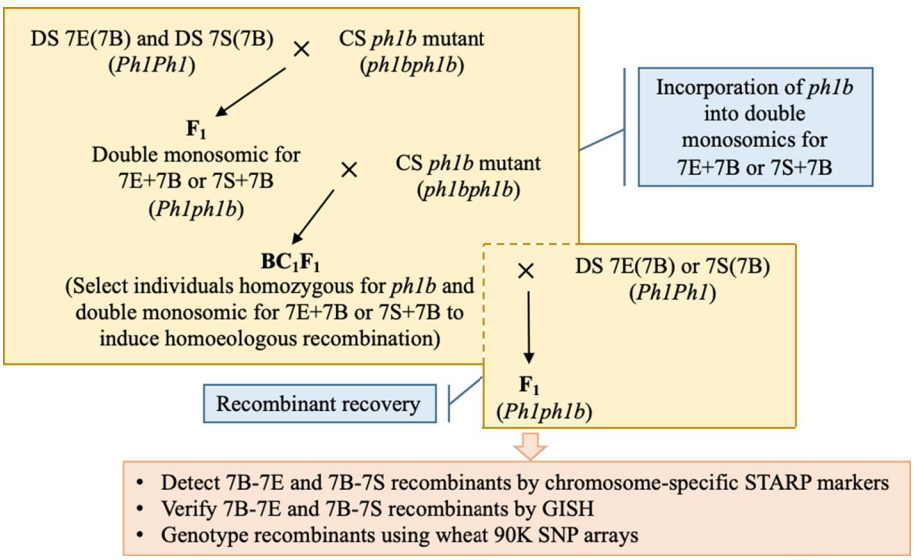

Fig. 1 Diagram showing induction, recovery, detection, and characterization of 7B − 7E and 7B − 7S homoeologous recombinants

to analyze and call SNP clusters (Illumina Inc., San Diego, CA, USA) as described by Zhang et al. (2018b).

Cytogenetic analysis

Fluorescent genomic in situ hybridization (GISH) was performed to differentiate *Ae. speltoides* and *Th. elongatum* chromatin from wheat chromatin as described by Cai et al. (1998). Total genomic DNA of *Ae. speltoides* and *Th. elongatum* was used as GISH probes and was labeled with Bio-16-dUTP by nick translation (Enzo Life Science, Inc., USA). Total CS genomic DNA was used as blocking after being sheered in boiling 0.4 M NaOH for 40–50 min. Hybridization signals on *Ae. speltoides* and *Th. elongatum* chromatin were detected with fluorescein isothiocyanate-conjugated avidin (FITC-avidin) (Vector Laboratories, Inc., USA) as green–yellow, and wheat chromatin was counter-stained with propidium iodide (PI) as red.

Microscopy

A fluorescence microscope (BX51, Olympus, Japan) with a CCD camera (DP72, Olympus, Japan) was used to visualize the GISH signals and chromosomes. GISH images were captured by Olympus CellSens software.

Results

Development and validation of chromosome-specific STARP markers for the detection of 7B – 7E and 7B – 7S recombinants

The wheat 90 K SNP assay mapped 2347 SNPs to wheat chromosome 7B (Wang et al. 2014). Out of these mapped SNPs, we identified 1018 polymorphic for the homoeologous pair 7B – 7S (Zhang et al. 2018a, b) and 1055 polymorphic for 7B – 7E. Initially, the polymorphic SNPs, physically mapped to the pericentromeric and distal regions on both arms of chromosome 7B, were used as queries to search against the IWGSC RefSeq v2.0 and the *Ae. speltoides* genome sequences (https://wheat-urgi.versailles.inra.fr/), and *Th. elongatum* RNA-Seq database (http://blast.ncbi.nlm.nih.gov/blast/Blast.cgi) by BLASTn. The SNPs polymorphic between 7B and 7E or 7B and 7S, and also polymorphic between 7B/7S/7E and 7A/7D were ideal for the development of STARP markers diagnostic for the homoeologous pairs 7B – 7E and 7B – 7S. However, most of the 90 K SNPs within the targeted regions were found to be polymorphic for the homoeologous pair 7B – 7E or 7B – 7S, but not polymorphic between 7B/7S/7E and 7A/7D. Under this circumstance, we searched for new SNPs nearby the 90 K SNP loci within the targeted region on chromosome 7B by BLASTn and performed sequence alignment analysis to identify the SNPs diagnostic for the homoeologous pair 7B – 7E or 7B – 7S in the CS wheat background.

Four and eleven diagnostic STARP markers were developed for the homoeologous pair 7B – 7E and 7B – 7S, respectively (Table 1). They were located either within the pericentromeric region on the long arm or the terminal region on the short or long arm. Three 7B – 7E specific markers (*Xwgc2300*, *Xwgc2301*, and *Xwgc2303*) and three 7B – 7S specific markers (*Xwgc2304*, *Xwgc2307*, and *Xwgc2313*) were selected to pre-screen the homoeologous recombination population for 7B – 7E and 7B – 7S recombinants, respectively. They resided within the terminal region of the short arm, pericentromeric region on the long arm, and terminal region of the long arm in each of these two homoeologous pairs (Table 1 and Fig. 3a). *Xwgc2304* and *Xwgc2307* are codominant markers, and *Xwgc2313* is dominant for the homoeologous pair 7B – 7S. *Xwgc2300*, *Xwgc2301*, and *Xwgc2303* are dominant markers for the homoeologous pair 7B – 7E (Fig. 3a).

Meanwhile, we identified six 7B – 7E and eighteen 7B – 7S recombinants by GISH to verify the utility of the chromosome-specific STARP markers in recombinant detection. Marker analysis of the GISH-delineated 7B – 7E and 7B – 7S recombinants provided clear genotyping results consistent with their GISH patterns in terms of recombination breakpoints and sizes of the recombinant segments (Fig. 3). Therefore, these STARP markers were diagnostic for differentiating wheat chromosome 7B from *Th. elongatum* chromosome 7E and *Ae. speltoides* chromosome 7S in the targeted regions, and useful in detecting the recombinants of 7B with 7E and 7S.

Pre-screening and verification of 7B – 7E and 7B – 7S recombinants and aberrations by STARP markers and GISH

The chromosome-specific STARP markers we developed for the homoeologous pairs 7B – 7E and 7B – 7S enabled quick pre-screening of large recombination populations for recombinants involving these two homoeologous pairs. We pre-screened 578 individuals from the 7B – 7E recombination population using the three STARP markers diagnostic for 7B – 7E (*Xwgc2300*, *Xwgc2301*, and *Xwgc2303*) and identified 116 individuals containing either a 7B – 7E recombinant chromosome or other structural aberration involving chromosome 7B. Similarly, 288 individuals from the 7B – 7S recombination population were pre-screened by the STARP markers diagnostic for 7B – 7S (*Xwgc2304*, *Xwgc2307*, and *Xwgc2313*). Seventy-nine of them were found to contain a 7B – 7S recombinant chromosome or other structural aberration involving chromosome 7B.

Table 1 SNP-derived STARP markers specific for the 7B – 7E and 7B – 7S homoeologous pairs

Markers	SNP alleles	SNP locations[a]	Forward and reverse primers[b]	Polymorphism
Xwgc2300	[A/G]	7BS (603,689 bp)	F1: [Tail 2]-5′ GACGATGACAGCTCCGCA 3′ F2: [Tail 1]-5′ GACGATGACAGATCCTCG 3′ R: 5′ CCAAGTTTGCAGAGGCAGAAG 3′	7B – 7E
Xwgc2301	[T/C]	7BL (379,299,483 bp)	F1: [Tail 2]-5′ AAAGCTGTCCGGTTTACTCTT 3′ F2: [Tail 1]-5′ AAAGCTGTCCGATTTGCCATC 3′ R: 5′ CGCATGCATGTGCGTGTA 3′	7B – 7E
Xwgc2302	[A/G]	7BL (386,081,398 bp)	F1: [Tail 2]-5′ CATTCTACCCTACGCACGTA 3′ F2: [Tail1]-5′ CATTCTACCCTACGCATACG 3′ R: 5′ CCATTTCCATTCCATTCAGGACAA	7B – 7E
Xwgc2303	[T/G]	7BL (758,280,973 bp)	F1: [Tail 2]-5′ CCAGGAGTCAACACAAAAT 3′ F2: [Tail 1]-5′ CCAGGAGTCAACACAAGAG 3′ R: 5′ GCACTCCGCCTCTGATGC 3′	7B – 7E
Xwgc2304	[C/A]	7BS (3,695,566 bp)	F1: [Tail 1]-5′ TATGCTCTTATTCGCGACC 3′ F2: [Tail 2]-5′ TATGCTCTTATTCGCGGTA 3′ R: 5′ GCGTACGTCAATCACGGATCAG 3′	7B – 7S
Xwgc2305	[A/G]	7BS (4,121,716 bp)	F1: [Tail 2]-5′ CGTAAGCAATGTAGTTTATATTGA 3′ F2: [Tail 1]-5′ CGTAAGCAATGTAGTTTATACCGG 3′ R: 5′ GAGAGTGGTCCCTGTCTGATG 3′	7B – 7S
Xwgc2306	[A/G]	7BS (244,368,635 bp)	F1: [Tail 1]-5′ GCAATAAAATATAACAATCAACAAAATAAA 3′ F2: [Tail 2]-5′ GCAATAAAATATAACAATCAACAAAACCAG 3′ R: 5′ GGTTTGCCGTTCTATCATATCAGC 3′	7B – 7S
Xwgc2307	[T/C]	7BL (379,299,435 bp)	F1: [Tail 2]-5′ GTCCATGGCATCACAACGT 3′ F2: [Tail 1]-5′ GTCCTTGGCATCACACAGC 3′ R: 5′ CAGCTTTGTTGCCACATTTCC 3′	7B – 7S
Xwgc2308	[A/G]	7BL (396,962,870 bp)	F1: [Tail 1]-5′ TCATTCATTTCATACAGAGACG 3′ F2: [Tail 2]-5′ TCATTCATTTCATACAGAAGCA 3′ R: 5′ CCAATGATGTTACTTTGATGCTGC 3′	7B – 7S
Xwgc2309	[A/G]	7BL (465,240,318 bp)	F1: [Tail 1]-5′ ACAAGGTGACAAGACTTCTCA 3′ F2: [Tail 2]-5′ ACAAGGTGACAAGACTTTCCG 3′ R: 5′ GGTTTGCCGTTCTATCATATCAGC 3′	7B – 7S
Xwgc2310	[A/G]	7BL (654,629,105 bp)	F1: [Tail 2]-5′ CCATATCGTAGCACATGAACGTA 3′ F2: [Tail 1]-5′ CCATATCGTAGCACATGAATATG 3′ R: 5′ TCTTCACTGTGGGTCGGCA 3′	7B – 7S
Xwgc2311	[G/T]	7BL (655,975,979 bp)	F1: [Tail 1]-5′ GACCACCTGTGTGTGTACATG 3′ F2: [Tail 2]-5′ GACCACCTGTGTGTGTAACTT 3′ R: 5′ CCCTACAACAACAAACAAAAGAACAT 3′	7B – 7S
Xwgc2312	[A/G]	7BL (754,572,320 bp)	F1: [Tail 1]-5′ TGACATGGGAGCCTAGG 3′ F2: [Tail 2]-5′ TGACATGGGAGCCCGGA 3′ R: 5′ CCCCAGGCAGACAATTCATTTT 3′	7B – 7S
Xwgc2313	[A/G]	7BL (754,572,989 bp)	F1: [Tail 2]-5′ ACTAAGACCCTGAACAAGCAAA 3′ F2: [Tail 1]-5′ ACTGAGACCCTGAACAAGTCAG 3′ R: 5′ CTGAATTCCACAGGAGATACCATTAA 3′	7B – 7S
Xwgc2314	[C/G]	7BL (754,570,889 bp)	F1: [Tail 1]-5′ AGAGGAAACGGGGCCCAC 3′ F2: [Tail 2]-5′ GGCTCGTCAGTGTACCTG 3′ R: 5′ GCTAAAGTATTTATTTATCCTCTGCCCA 3′	7B – 7S

[a]SNP locations in the IWGSC Reference Sequence v2.0 assembly (IWGSC RefSeq v2.0)

[b][Tail1] = GCAACAGGAACCAGCTATGAC; [Tail2] = GACGCAAGTGAGCAGTATGAC

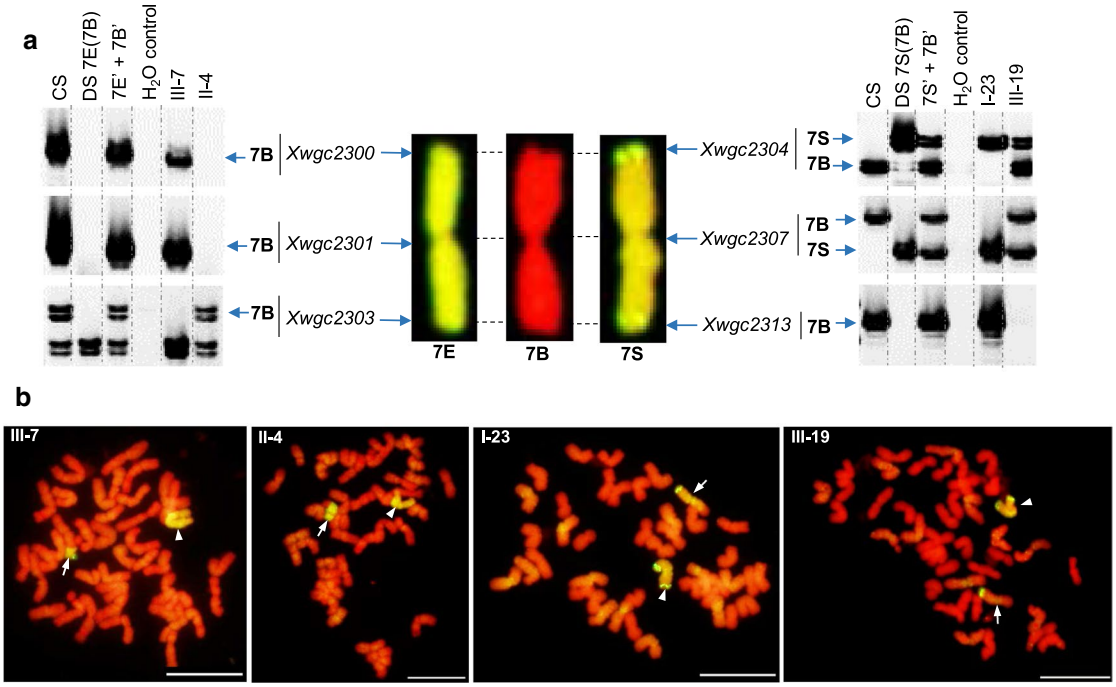

Fig. 3 Detection of 7B – 7E and 7B – 7S recombinants by chromosome-specific STARP markers (**a**) and verification of the recombinants by GISH (**b**). GISH painted wheat chromosomes/segments in red, and chromosome 7E and 7S and their segments in yellow–green. Arrows point to 7B – 7E or 7B – 7S recombinant chromosomes and arrowheads to chromosome 7E or 7S. III-7 and II-4 are 7B – 7E recombinants, designated 7BS·7BL – 7EL and 7ES·7EL – 7BL, respectively. I-23 and III-19 are 7B – 7S recombinants, designated 7SS·7SL – 7BLand 7BS·7BL – 7SL, respectively. Scale bar = 10 µm

The *ph1b* mutant induces homoeologous recombination of wheat chromosome 7B with *Th. elongatum* chromosome 7E and *Ae. speltoides* 7S, and with its wheat homoeologues 7A and 7D as well. In addition, other chromosome aberrations, including Robertsonian translocations, telocentric chromosomes, and chromosome deletions, could occur in the special genotypes constructed for homoeologous recombination induction. Therefore, we expected to see these chromosome aberrations in addition to 7B – 7E or 7B – 7S recombinants among the STARP marker-based selections. Thus, GISH was performed to verify chromosome constitutions of the preselected individuals. Out of 116 individuals preselected from the 7B – 7E recombination population, we detected 23 7B – 7E recombinants, seven Robertsonian translocations, and one telocentric chromosome of 7E. The rest 85 individuals were found to contain one or two copies of chromosome 7E without any GISH-detectable recombinants or chromosome aberrations involving 7E. They were preselected by the chromosome-specific STARP markers probably because their chromosome 7B recombined with chromosome 7A or 7D, leading to an absence of one or more segments tagged by the markers. Similarly, GISH analysis detected 43 7B – 7S recombinants, four Robertsonian translocations, and three deletions of chromosome 7S from the 79 individuals selected from the 7B – 7S recombination population. In addition, GISH detected two extra interstitial 7B – 7S recombination events (V-10 and V-11 in Fig. 4), which involved the regions not covered by the STARP markers. The other 29 selected individuals contained one or two copies of chromosome 7S and probably missed one or more marker-tagged segments on chromosome 7B.

The 7B – 7E and 7B – 7S recombinants and chromosome aberrations were placed into six categories, respectively, according to their GISH-revealed structural components (Fig. 4). A total of 29 7B – 7E and 61 7B – 7S recombinants were detected and verified by chromosome-specific markers and GISH (Table 2). The number of single crossover-derived 7B – 7S terminal recombinants containing a small 7B segment (Category 1) and a small 7S segment (Category 2) were 30 and 27, with a recombination rate of 6.88% and 6.19%, respectively (Fig. 4 and Table 2). The single crossover-derived 7B – 7E recombination rates for Category 1 and Category 2 were 2.48% and 2.02%, respectively, which were much lower than 7B – 7S. Two double crossover-derived (V-9 and V-12) and two multiple crossover-derived (V-10 and V-11) interstitial recombinants were detected for the homoeologous pair 7B – 7S, but not for 7B – 7E. In addition, we identified seven 7B – 7E Robertsonian translocations (1.09%) and one 7E telocentric chromosome (0.16%) from the 7B – 7E recombination population, and four 7B – 7S

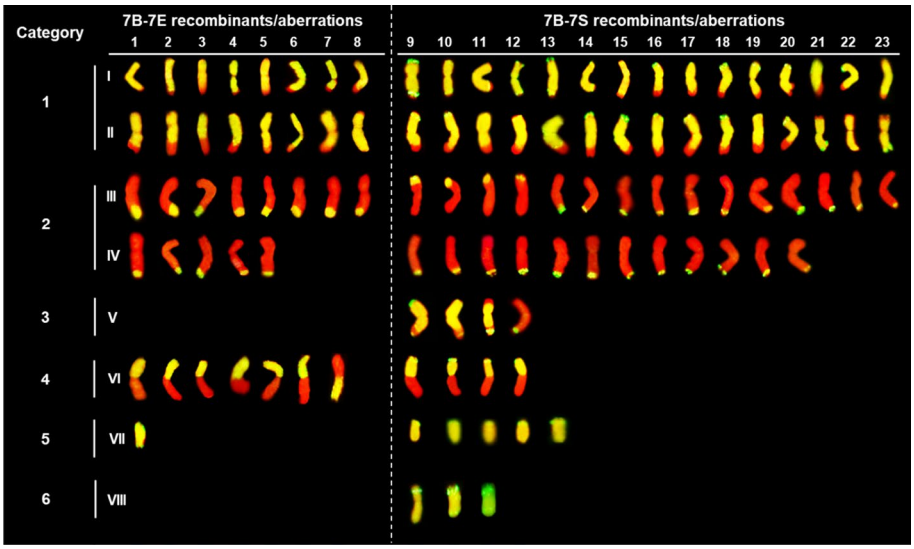

Fig. 4 GISH-painted 7B-7E and 7B-7S recombinant chromosomes and aberrations in six categories, including **Category 1** (I & II)—terminal recombinants with a small 7B segment, **Category 2** (III & IV)—terminal recombinants with a small 7E or 7S segment, **Category 3** (V) -interstitial recombinants, **Category 4** (VI)—Robertsonian translocation, **Category 5** (VII) -telocentric 7E or 7S chromosomes, and **Category 6** (VIII)—chromosome 7E or 7S deletions. Chromosome 7B segments were painted in red, and 7E and 7S chromosome segments in yellow-green

Table 2 The frequencies of different 7B – 7E and 7B – 7S recombinants and aberrations

Homoeologous pairs	No. individuals screened	Recombinants			Misdivision products		Deletions
		Category 1	Category 2	Category 3	Category 4	Category 5	Category 6[a]
7B – 7E	644	16	13	0	7	1	0
		2.48%	2.02%	0.00%	1.09%	0.16%	0.00%
7B – 7S	436	30	27	4	4	5	3
		6.88%	6.19%	0.92%	0.92%	1.14%	0.69%

[a]See Fig. 4 for detailed description of these six categories of recombinants and aberrations

Robertsonian translocations (0.92%) and five 7S telocentric chromosomes (1.14%) from the 7B – 7S recombination population. Also, the long arm deletions of chromosome 7S (0.69%) were identified from the 7B – 7S recombination population, including VIII-9, VIII-10, and VIII-11 (Fig. 4). Most of the 7B – 7E and 7B – 7S recombinants involved their long arms. Only one recombination event was recovered in the short arm of the homoeologous pair 7B – 7E (II-8) and eight in the short arm of 7B – 7S (II-21–23, III-9–12, and V-11) (Fig. 4; Supplementary 1). The detailed compositions and pedigrees of all 7B – 7E and 7B – 7S recombinants and aberrations are provided in Supplementary 1.

Homoeologous recombination-based delineation and dissection of wheat chromosome 7B

The 7B – 7E and 7B – 7S recombinants were genotyped together with several controls, including CS, DS 7E(7B), DS 7S(7B), and double monosomics 7E' + 7B' and 7S' + 7B', using wheat 90 K SNP arrays. Out of 2347 SNPs mapped to wheat chromosome 7B (Wang et al. 2014), we identified 430 SNPs polymorphic for the homoeologous pair 7B – 7E and 352 for 7B – 7S. The 7B – 7E and 7B – 7S homoeologous pairs shared 241 polymorphic SNPs. In total, 541 wheat 90 K SNPs were polymorphic for the homoeologous pairs 7B – 7E and 7B – 7S, with 189 SNPs specifically for 7B – 7E and 111 for 7B – 7S (Fig. 5a). Overall, the homoeologous pair 7B – 7E had a higher level of polymorphism than 7B – 7S at the 90 K SNP loci.

The SNPs polymorphic for the homoeologous pair 7B – 7E and 7B – 7S genetically mapped to chromosome 7B (Wang et al. 2014). We physically aligned the SNP loci onto chromosome 7B by BLASTn against the IWGSC RefSeq v2.0 (https://wheat-urgi.versailles.inra.fr/) (Supplementary 2). The sequenced wheat 7B chromosome size in the IWGSC RefSeq v2.0 was 763.71 Mb, which covered 85.91% of the entire chromosome 7B (889 Mb) (https://wheat-urgi.versailles.inra.fr/; Šafář et al. 2010). The genetic and physical positions of the SNPs were plotted as an "S" curve distribution (Fig. 5b). The average cM/Mb ratio along the entire chromosome was 0.25. The SNPs within the linkage block of 67.47–78.44 cM, which traverses the centromere, span the physical region of 118.71–589.04 Mb, with an average cM/Mb ratio of 0.023. Thus, the homoeologous recombination rate in the proximal region was significantly lower than the distal region for the homoeologous pairs 7B – 7E and 7B – 7S.

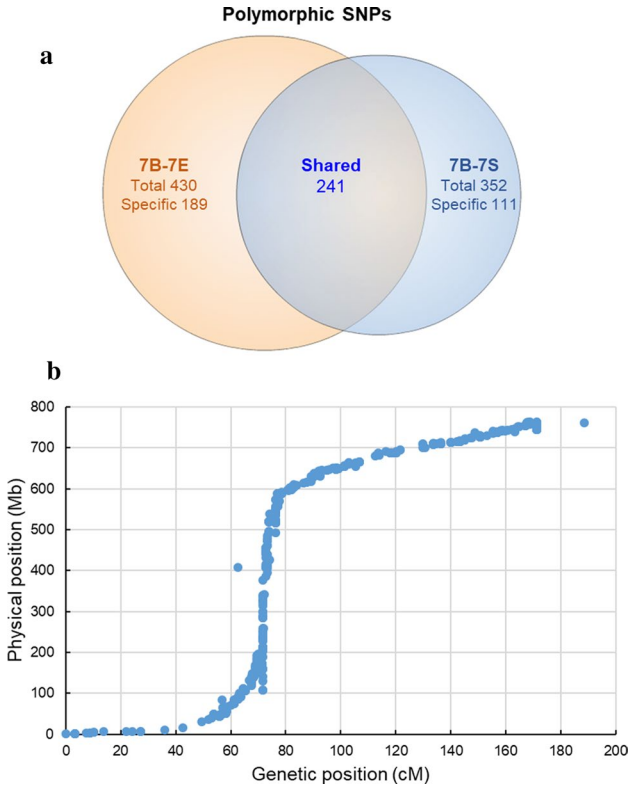

Fig. 5 Polymorphic SNPs of the homoeologous pair 7B – 7E and 7B – 7S (**a**) and their genetic and physical positions on chromosome 7B (**b**)

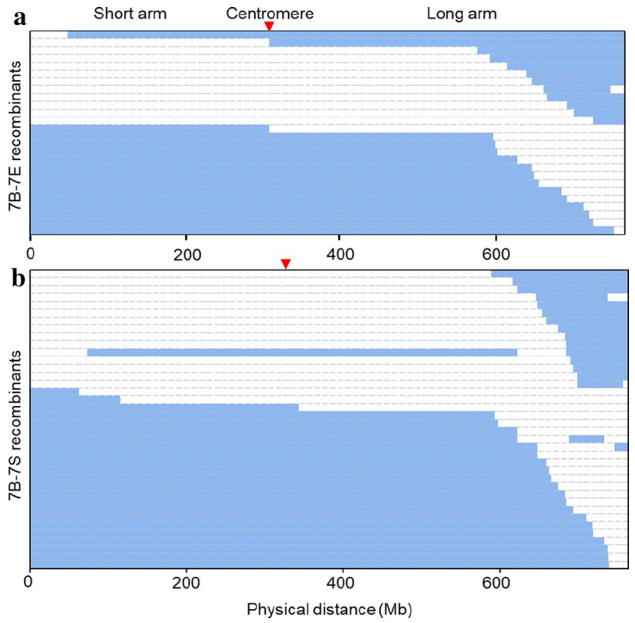

Fig. 6 Graphical representation of the 26 7B – 7E recombinants (*top*) and 38 7B – 7S recombinants (*bottom*), showing their SNP genotypes and GISH patterns. Blue bars represent chromosome 7E or 7S segments and open bars for 7B segments. Red triangles point to the centromere positions

Overall, the wheat 90 K SNP genotyping results of the 7B – 7E and 7B – 7S recombinants were consistent with their GISH patterns except for a few discrepancies. Wheat 90 K SNP genotyping identified IV-1 as an interstitial 7B – 7E recombinant with a small 7E segment proximal to a 7BL terminal segment on the long arm. However, the 7BL terminal segment in IV-1 was not detected by GISH (Fig. 4; Supplementary 3). IV-20 was initially identified as a 7B – 7S terminal recombinant with a small 7S segment at the end of the long arm by GISH. But, wheat 90 K SNP genotyping detected a terminal 7B segment distal to the 7S segment on the long arm, identifying it as an interstitial 7B – 7S recombinant (Fig. 4; Supplementary 3). Some of the 7B – 7E and 7B – 7S recombinants had similar GISH patterns and could not be resolved by SNPs. Only one of the recombinants with the same SNP genotype was used for delineation and dissection analysis. Thus, we selected 26 representative 7B – 7E recombinants involving 23 unique recombination breakpoints and 38 representative 7B – 7S recombinants involving 31 unique breakpoints to partition wheat chromosome 7B. The integrative SNP and GISH analysis of the 7B – 7E and 7B – 7S recombinants resolved their recombination breakpoints and segment sizes. Consequently, wheat chromosome 7B was physically partitioned and dissected by these homoeologous recombination events. The overall results about 7B – 7E and 7B – 7S recombination-based partition and dissection of wheat chromosome 7B are graphically illustrated in Fig. 6. The physical locations of the recombination breakpoints were estimated as the middle point between the SNP loci immediately flanking the breakpoint (Supplementary 3). Most of the 7B – 7E and 7B – 7S recombination breakpoints clustered in the distal regions of the long arm (Fig. 6).

Construction of the composite bin map for wheat chromosome 7B

Chromosome 7B was partitioned into 24 bins with 430 SNPs assigned based on the GISH patterns and SNP genotyping data of the 26 representative 7B – 7E recombinants. Likewise, chromosome 7B was partitioned into 32 bins with 352 SNPs assigned based on the SNP data and GISH patterns of the 38 representative 7B – 7S recombinants. A composite bin map was constructed for chromosome 7B individually based on the 7B – 7E and 7B – 7S recombination, respectively (Supplementary 4). In addition, we integrated the SNP data and GISH patterns of all representative 7B – 7E and 7B – 7S recombinants to construct an integrative composite bin map for wheat chromosome 7B. The integrated genetic and physical analysis with the reference of the IWGSC

RefSeq v2.0 (https://wheat-urgi.versailles.inra.fr/) led to an informative composite bin map containing 44 distinct bins and 523 SNPs (Fig. 7). The estimated bin size ranged from 0.84 to 266.74 Mb, and the number of SNPs assigned to each of the bins ranged from 1 to 107 (Supplementary 5). The pericentromeric bins were significantly larger than others toward the distal regions on both arms, indicating lower recombination near the centromeric regions than in other chromosomal regions for the homoeologous pairs 7B – 7E and 7B – 7S.

Discussion

Meiotic homoeologous recombination generates genetically compensating recombinants for genome studies and expands genetic diversity of wheat and its relatives. Recent advances in genomics and associated technologies have dramatically increased the efficacy and throughput of homoeologous recombination-based chromosome engineering in alien introgression and provide a unique approach of investigating the complex polyploid genome of wheat (Niu et al. 2011a, b; Zhao et al. 2013; Zhang et al. 2015, 2017, 2018a, b, 2019, 2020; Danilova et al. 2017; King et al. 2018; Dai et al. 2020; Grewal et al. 2020). The availability of the wheat reference genome sequence IWGSC RefSeq v2.0 (https://wheat-urgi.versailles.inra.fr/) and the genome sequences of *Ae. speltoides* and *Th. elongatum* permitted us to survey the polymorphisms of wheat chromosome 7B with its homoeologous counterparts 7S in *Ae. speltoides* and 7E in *Th. elongatum* for chromosome-specific marker development. Through that approach, we identified homoeoalleles at multiple SNP loci diagnostic for the pericentromeric and distal regions on both arms of the homoeologous pairs 7B – 7E and 7B – 7S. The chromosome-specific STARP markers developed from the diagnostic SNPs tagged the critical homoeologous regions of chromosomes 7B, 7E, and 7S, allowing for quick prescreening of large recombination populations for 7B – 7E and 7B – 7S recombinants. Thus, chromosome-specific DNA markers enable homoeologous recombination-based chromosome engineering in a large scale and improved efficacy. We induced and recovered a total of 29 7B – 7E and 61 7B – 7S recombinants using this genomics-enabled chromosome engineering technology. Integrative SNP and GISH analysis of the recombinants partitioned wheat chromosome 7B into 44 distinct bins with 523 SNPs assigned within, providing a unique homoeologous recombination-based physical framework for wheat genome study. Overall, the homoeologous pair 7B – 7S had a significantly higher recombination rate than 7B – 7E. Also, multiple crossover-derived recombinants were recovered for 7B – 7S, but not for 7B – 7E. In addition, SNP analysis indicated that the homoeologous pair 7B – 7S had lower polymorphism than 7B – 7E. All these results suggest that wheat chromosome 7B has a higher homology with *Ae. speltoides* chromosome 7S than with *Th. elongatum* chromosome 7E.

The majority of 7B – 7E and 7B – 7S recombination events clustered in the distal and sub-distal regions of these two homoeologous pairs. No 7B – 7E and 7B – 7S recombination events were recovered within the large pericentromeric region (> 1/2 the physical length of the entire chromosome 7B) (Fig. 7). Also, we observed extremely low recombination frequency in the short arms of both homoeologous pairs, especially for 7B – 7E. This might result from the 4AL/7BS translocation in wheat, where the terminal segment of 7BS was translocated to the terminal region of 4AL

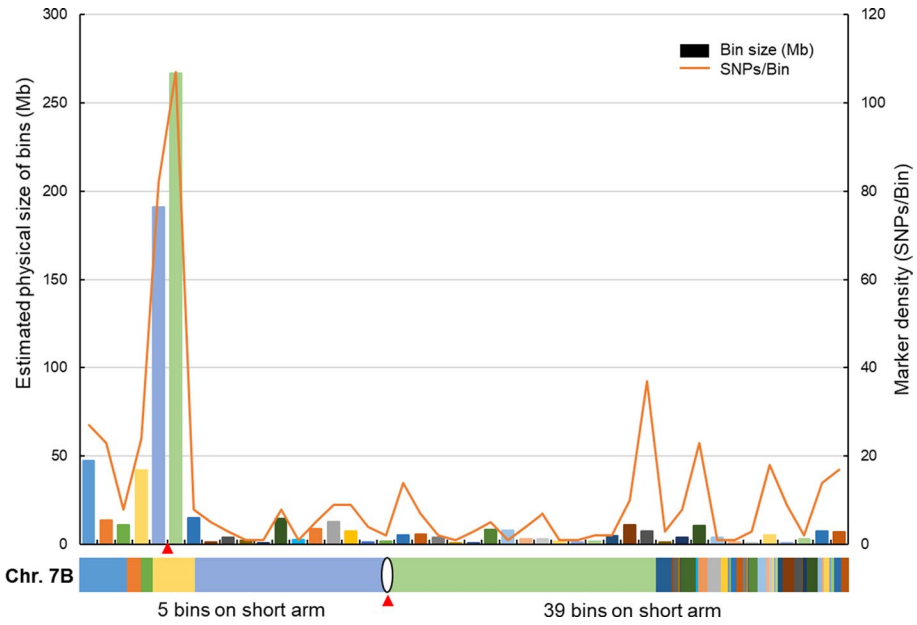

Fig. 7 Composite bin map of wheat chromosome 7B and corresponding partitioned chromosome 7B. Vertical bars indicate physical size of the bins, and curved lines indicate SNP numbers within each bin. All bins were color-coded according to their physical size and locations in the horizontal ideogram of chromosome 7B (*bottom*). The red triangle points to the centromere

(Devos et al. 1995; Miftahudin et al. 2004). Apparently, the absence of the terminal region on 7BS limited its recombination with the homoeologous regions on 7E and 7S.

The *ph1b* mutant induces meiotic homoeologous recombination between wheat and alien chromosomes, and between homoeologous chromosomes from different wheat subgenomes (A, B, and D) as well. In this study, we used the *ph1b* mutant to induce 7B – 7E and 7B – 7S recombination under the double monosomic conditions (i.e., 7B' + 7E' and 7B' + 7S'). This should enhance homoeologous recombination of chromosome 7B with 7E and 7S as expected. However, chromosome 7B under a monosomic condition (i.e., 7B') might occasionally recombine with 7A" or 7D" by forming a heteromorphic trivalent during meiotic pairing. Similarly, chromosome 7E or 7S could occasionally recombine with the homologous chromosome pair 7A" or 7D". Also, we found that chromosome aberrations, including Robertsonian translocation, telocentric chromosomes, and deletions, occurred in the special genotypes. These untargeted homoeologous recombination and chromosome aberrations complicated the marker-based pre-screening for recombinants and led to false preselection of the recombinants. We identified 23 7B – 7E recombinants from 116 individuals preselected by STARP markers and 43 7B – 7S recombinants from 79 preselected individuals. Some of the preselected individuals were verified by GISH as chromosome aberrations involving 7B and 7S or 7E, including 7B – 7S and 7B – 7E Robertsonian translocations, telocentric chromosomes, and deletions. Most likely, 7B – 7S and 7B – 7E Robertsonian translocations and telocentric chromosomes resulted from centric misdivision of the univalent chromosomes 7B', 7E', and 7S'. Fusion of the misdivision products (i.e., telocentric chromosomes) resulted in 7B – 7S and 7B – 7E Robertsonian translocations (Friebe et al. 2005). In addition, some of the preselected individuals contained one or two copies of chromosome 7E or 7S without any GISH-detectable recombinants and aberrations involving chromosome 7E or 7S. They were selected in the STARP marker-based pre-screening due probably to the absence of the chromosome 7B-specific marker alleles caused by homoeologous recombination of chromosome 7B with 7A or 7D. The deletions might be induced by the *Ae. speltoides*-derived gametocidal gene (Tsujimoto and Tsunewaki 1988).

Both homologous and homoeologous recombination can be resolved by DNA markers. But, only homoeologous recombination can be visualized by GISH, making it unique for genome study. We took this advantage of homoeologous recombination to partition wheat chromosome 7B for physical mapping by performing integrative marker and GISH analysis of the 7B – 7E and 7B – 7S recombinants. The composite bin map of chromosome 7B constructed through this approach provided a unique physical framework for the complex polyploid genome of wheat. However, this homoeologous recombination-based chromosome mapping may confront limitations imposed by the physical coverage of markers on the targeted chromosomes and resolution of GISH in chromatin detection. In this study, we identified a total of 29 7B – 7E and 61 7B – 7S recombinants. Some of the recombinants with close recombination breakpoints could not be distinguished from each other by GISH. Also, they could not be resolved by the wheat 90 K SNP genotyping assay due to the lack of diagnostic SNPs within the chromosomal regions flanking the breakpoints. In these cases, we used only one of those recombinants for chromosome mapping. Thus, increasing marker coverage on the recombination chromosomes can make the similar recombinants more resolvable and consequently improve the resolution of homoeologous recombination-based chromosome mapping. On the other hand, small recombination segments, which cannot be visualized by GISH, may be detectable by the diagnostic markers tagging the segments. For instance, the wheat 90 K SNP genotyping assay detected a tiny 7BL terminal segment in the 7B – 7E recombinant chromosome of IV-1 and in the 7B – 7S recombinant chromosome of IV-20, respectively. However, both terminal segments were too small to be visualized by GISH (Fig. 4; Supplementary 3). In the same manner, GISH might be able to detect the recombination segments that are not resolvable by markers due to the lack of diagnostic markers within the chromosomal region involved in the recombination, such as the interstitial recombination segments in the 7B – 7S recombinants V-10 and V-11 (Fig. 4) and the homoeologous recombination reported by Zhang et al. (2020).

In summary, we physically dissected wheat chromosome 7B by homoeologous recombination-based chromosome engineering and developed a unique physical framework of chromosome 7B useful for wheat genome study. In addition, the 7B – 7E and 7B – 7S recombinants diversify and enrich the wheat genome and represent a useful gene source for wheat improvement. The genomics-enabled chromosome engineering pipeline we developed in this study will further facilitate homoeologous recombination-based genome studies and alien introgression in wheat improvement.

Acknowledgements We thank Mary Osenga for her help in high-throughput SNP genotyping and Drs. Lili Qi and Rebekah Oliver for their critical review of the manuscript. This project has been supported by Agriculture and Food Research Initiative Competitive Grant No. 2013-67013-21121 and 2019-67013-29164 from the USDA National Institute of Food and Agriculture.

Author contributions M.Z. contributed to recombinant production and analysis, SNP assays, GISH, molecular marker development and analysis, and chromosome mapping, and was involved in data analysis and manuscript preparation. W.Z. and X.Z. participated in crossing, chromosome-specific marker analysis, and GISH. Q.S. and C.Y. analyzed

DNA sequence data. J.F. ran high-throughput SNP assays. S.S.X. was involved in manuscript preparation. X.C. designed and coordinated this work, and was involved in crosses, data analysis and interpretation, and manuscript preparation.

Compliance with ethical standards

Conflict of interest The authors declare that they have no conflict of interest.

References

Avni R, Nave M, Barad O, Baruch K, Twardziok SO, Gundlach H, Hale L, Mascher M, Spannagl M, Wiebe K, Jordan KW, Golan G, Deek J, Ben-Zvi G, Himmelbach A, MacLachlan RP, Sharpe AG, Fritz A, Ben-David R, Budak H, Fahima T, Korol A, Faris JD, Hernandez A, Mikel MA, Levy AA, Steffenson B, Maccaferri M, Tuberosa R, Cattivelli L, Faccioli P, Ceriotti A, Kashkush K, Pourkheirandish M, Komatsuda T, Eilam T, Sela H, Sharon A, Ohad N, Chamovitz DA, Mayer KFX, Stein N, Ronon G, Peleg Z, Pozniak CJ, Akhunov ED, Distelfeld A (2017) Wild emmer genome architecture and diversity elucidate wheat evolution and domestication. Science 357:93–97

Cai X, Jones S, Murray T (1998) Molecular cytogenetic characterization of *Thinopyrum* and wheat–*Thinopyrum* translocated chromosomes in a wheat *Thinopyrum* amphiploid. Chromosome Res 6:185–189

Chen PD, Qi LL, Zhou B, Zhang SZ, Liu DJ (1995) Development and molecular cytogenetic analysis of wheat-*Haynaldia villosa* 6VS/6AL translocation lines specifying resistance to powdery mildew. Theor Appl Genet 91:1125–1128

Chen P, Liu W, Yuan J, Wang X, Zhou B, Wang S, Zhang S, Feng Y, Yang B, Liu G, Liu D, Qi L, Zhang P, Friebe B, Gill BS (2005) Development and characterization of wheat-*Leymus racemosus* translocation lines with resistance to *Fusarium* Head Blight. Theor Appl Genet 111:941–948

Crasta OR, Francki MG, Bucholtz DB, Sharma HC, Zhang J, Wang RC, Ohm HW, Anderson JM (2000) Identification and characterization of wheat-wheatgrass translocation lines and localization of barley yellow dwarf virus resistance. Genome 43:698–706

Dai K, Zhao R, Shi M, Xiao J, Yu Z, Jia Q, Wang Z, Yuan C, Sun H, Cao A, Zhang R, Chen P, Li Y, Wang H, Wang X (2020) Dissection and cytological mapping of chromosome arm 4VS by the development of wheat-*Haynaldia villosa* structural aberration library. Theor Appl Genet 133:217–226

Danilova TV, Friebe B, Gill BS (2014) Development of a wheat single gene FISH map for analyzing homoeologous relationship and chromosomal rearrangements within the Triticeae. Theor Appl Genet 127:715–730

Danilova TV, Zhang G, Liu W, Friebe B, Gill BS (2017) Homoeologous recombination-based transfer and molecular cytogenetic mapping of a wheat streak mosaic virus and *Triticum* mosaic virus resistance gene *Wsm3* from *Thinopyrum intermedium* to wheat. Theor Appl Genet 130:549–556

Danilova TV, Friebe B, Gill BS (2019) Production of a complete set of wheat-barley group-7 chromosome recombinants with increased grain β-glucan content. Theor Appl Genet 132:3129–3141

Devos KM, Dubcovsky J, Dvorak J, Chinoy CN, Gale MD (1995) Structural evolution of wheat chromosomes 4A, 5A, and 7B and its impact on recombination. Theor Appl Genet 91:282–288

Endo TR, Gill BS (1996) The deletion stocks of common wheat. J Hered 87:295–307

Faris JD (2014) Wheat domestication: key to agricultural revolutions past and future. In: Tuberosa R, Graner A, Frison E (eds) Genomics of plant genetic resources. Vol. 1. Managing, sequencing and mining genetic resources. Springer, Netherlands, pp 439–464

Feldman M, Levy AA (2012) Genome evolution due to allopolyploidization in wheat. Genetics 192:763–774

Friebe B, Jiang J, Raupp WJ, Mclntosh RA, Gill BS (1996) Characterization of wheat-alien translocations conferring resistance to diseases and pests: current status. Euphytica 91:59–87

Friebe B, Zhang P, Linc G, Gill BS (2005) Robertsonian translocations in wheat arise by centric misdivision of univalents at anaphase I and rejoining of broken centromeres during interkinesis of meiosis II. Cytogenet Genome Res 109:293–297

Friebe B, Qi L, Liu C, Gill B (2011) Genetic compensation abilities of *Aegilops speltoides* chromosomes for homoeologous B-genome chromosomes of polyploid wheat in disomic S(B) chromosome substitution lines. Cytogenet Genome Res 134:144–150

Gill KS, Gill BS (1991) A DNA fragment mapped within the submicroscopic deletion of *Ph1*, a chromosome pairing regulator gene in polyploid wheat. Genetics 129:257–259

Gyawali Y, Zhang W, Chao S, Xu SS, Cai X (2019) Delimitation of wheat *ph1b* deletion and development of the *ph1b*-specific DNA markers. Theor Appl Genet 132:195–204

Grewal S, Hubbart-Edwards S, Yang C, Devi U, Baker L, Heath J, Scholefield SAD, Howells C, Yarde J, Isaac P, King IP, King J (2020) Rapid identification of homozygosity and site of wild relative introgressions in wheat through chromosome-specific KASP genotyping assays. Plant Biotechnol J 18:743–755

International Wheat Genome Sequencing Consortium (IWGSC) (2018) Shifting the limits in wheat research and breeding using a fully annotated reference genome. Science 361:6403

King J, Grewal S, Yang CY, Hubbart Edwards S, Scholefield D, Ashling S, Harper JA, Allen AM, Edwards KJ, Burridge AJ, King IP (2018) Introgression of *Aegilops speltoides* segments in *Triticum aestivum* and the effect of the gametocidal genes. Ann Bot 121:229–240

Li H, Dong Z, Ma C, Tian X, Qi Z, Wu N, Friebe B, Xiang Z, Xia Q, Liu W, Li T (2019) Physical mapping of stem rust resistance gene *Sr52* from *Dasypyrum villosum* based on *ph1b*-induced homoeologous recombination. Int J Mol Sci 20:4887

Ling H, Ma B, Shi X, Liu H, Dong L, Sun H, Cao Y, Gao Q, Zheng S, Li Y, Yu Y, Du H, Qi M, Li Y, Lu H, Yu H, Cui Y, Wang N, Chen C, Wu H, Zhao Y, Zhang J, Li Y, Zhou W, Zhang B, Hu W, van Eijk MJT, Tang J, Witsenboer HMA, Zhao S, Li Z, Zhang A, Wang D, Liang C (2018) Genome sequence of the progenitor of wheat A subgenome *Triticum urartu*. Nature 557:424–428

Liu W, Danilova TV, Rouse MN, Bowden RL, Friebe B, Gill BG (2013) Development and characterization of a compensating wheat-*Thinopyrum intermedium* Robertsonian translocation with *Sr44* resistance to stem rust (Ug99). Theor Appl Genet 126:1167–1177

Long Y, Chao WS, Ma G, Xu SS, Qi L (2017) An innovative SNP genotyping method adapting to multiple platforms and throughputs. Theor Appl Genet 130:597–607

Lukaszewski A, Rybka K, Korzun V, Malyshev S, Lapinski B, Whitkus R (2004) Genetic and physical mapping of homoeologous recombination points involving wheat chromosome 2B and rye chromosome 2R. Genome 47:36–45

Luo M, Gu YQ, Puiu D, Wang H, Twardziok SO, Deal KR, Huo X, Zhu T, Wang L, Wang Y, McGuire PE, Liu S, Long H, Ramasamy RK, Rodriguez JC, Van SL, Yuan L, Wang Z, Xia Z, Xiao L, Anderson OD, Ouyang S, Liang Y, Zimin AV, Pertea G, Qi P, Bennetzen JL, Dai X, Dawson MW, Müller H, Kugler K, Rivarola-Duarte L, Spannagl M, Mayer KFX, Lu F, Becan MW, Lerou P, Li P, You FM, Sun Q, Liu Z, Lyons E, Wicher T, Zalzberg SL, Devos KM, Dvořák J (2017) Genome sequence of the progenitor of the wheat D genome *Aegilops tauschii*. Nature 551:498–502

Mago R, Spielmeyer W, Lawrence G, Lagudah E, Ellis J, Pryor A (2002) Identification and mapping of molecular markers linked to rust resistance genes located on chromosome 1RS of rye using wheat-rye translocation lines. Theor Appl Genet 104:1317–1324

Miftahudin RK, Ross K, Ma XF, Mahmoud AA, Layton J, Milla MA, Chikmawati T, Ramalingam J, Feril O, Pathan MS, Momirovic GS, Kim S, Chema K, Fang P, Haule L, Struxness H, Birkes J, Yaghoubian C, Skinner R, McAllister J, Nguyen V, Qi LL, Echalier B, Gill BS, Linkiewicz AM, Dubcovsky J, Akhunov ED, Dvorák J, Dilbirligi M, Gill KS, Peng JH, Lapitan NL, Bermudez-Kandianis CE, Sorrells ME, Hossain KG, Kalavacharla V, Kianian SF, Lazo GR, Chao S, Anderson OD, Gonzalez-Hernandez J, Conley EJ, Anderson JA, Choi DW, Fenton RD, Close TJ, McGuire PE, Qualset CO, Nguyen HT, Gustafson JP (2004) Analysis of expressed sequence tag loci on wheat chromosome group 4. Genetics 168:651–663

Naranjo T, Fernández-Rueda P (1996) Pairing and recombination between individual chromosomes of wheat and rye in hybrids carrying the *ph1b* mutation. Theor Appl Genet 93:242–248

Neelam K, Brown-Guedira G, Huang L (2013) Development and validation of a breeder-friendly KASPar marker for wheat leaf rust resistance locus *Lr21*. Mol Breed 31:233–237

Niu Z, Klindworth DL, Friesen TL, Chao S, Jin Y, Cai X, Xu SS (2011) Targeted introgression of a wheat stem rust resistance gene by DNA marker-assisted chromosome engineering. Genetics 187:1011–1021

Niu Z, Klindworth DL, Yu G, Friesen TL, Chao S, Jin Y, Cai X, Ohm J-B, Rasmussen JB, Xu SS (2014) Development and characterization of wheat lines carrying stem rust resistance gene *Sr43* derived from *Thinopyrum ponticum*. Theor Appl Genet 129:969–980

Patokar C, Sepsi A, Schwarzacher T, Kishii M, Heslop-Harrison JS (2016) Molecular cytogenetic characterization of novel wheat-*Thinopyrum bessarabicum* recombinant lines carrying intercalary translocations. Chromosoma 125:163–172

Pont C, Leroy T, Seidel M, Tondelli A, Duchemin W, Armisen D, Lang D, Bustos-Korts D, Goué N, Balfourier F, Molnar-Lang M, Lage J, Kilian B, Ozkan H, Waite D, Dyer S, Alaux M, Letellier T, Russell J, Keller B, Eeuwijk F, Spannagl M, Mayer K, Waugh R, Stein N, Cattivelli L, Haberer G, Charmet G, Salse J (2019) Tracing the ancestry of modern bread wheats. Nat Genet 51:905–911

Qi L, Echalier B, Friebe B, Gill B (2003) Molecular characterization of a set of wheat deletion stocks for use in chromosome bin mapping of ESTs. Funct Integr Genom 3:39–55

Qi LL, Friebe B, Zhang P, Gill BS (2007) Homoeologous recombina-tion, chromosome engineering and crop improvement. Chromo-some Res 15:3–19

Rabinovich S (1998) Importance of wheat-rye translocations for breeding modern cultivar of *Triticum aestivum* L. Euphytica 100:323–340

Rey M, Calderón M, Prieto P (2015) The use of the *ph1b* mutant to induce recombination between the chromosomes of wheat and barley. Front Plant Sci. https://doi.org/10.3389/fpls.2015.00160

Riley R, Chapman V (1958) Genetic control of the cytologically diploid behaviour of hexaploid wheat. Nature 182:713–715

Riley R, Chapman V, Kimber G (1959) Genetic control of chromosome pairing in intergeneric hybrids with wheat. Nature 185:1244–1246

Riley R, Chapman V, Johnson R (1968) Introduction of yellow rust resistance of *Aegilops comosa* into wheat by genetically induced homoeologous recombination. Nature 217:383–384

Roberts MA, Reader SM, Dalgliesh C, Miller TE, Foote TN, Fish LJ, Snape JW, Moore G (1999) Induction and characterization of *Ph1* wheat mutants. Genetics 153:1909–1918

Šafář J, Šimková H, Kubaláková M, Číhalíková J, Suchánková P, Bartoš J, Doležel J (2010) Development of chromosome-specific BAC resources for genomics of bread wheat. Cytogenet Genome Res 129:211–223

Schwarzacher T, Anamthawat-Jónsson K, Harrison GE, Islam AKMR, Jia JZ, King IP, Leitch AR, Miller TE, Reader SM, Rogers WJ, Shi M, Heslop-Harrison JS (1992) Genomic in situ hybridization to identify alien chromosomes and chromosome segments in wheat. Theor Appl Genet 84:365–375

Sears ER (1954) The aneuploids of common wheat. Mo Agric Exp Stn Res Bull 572:1–59

Sears ER (1966) Nullisomic-tetrasomic combinations in hexaploid wheat. In: Riley R, Lewis KR (eds) Chromosome manipulation and plant genetics. Oliver and Boyd, Edinburgh, pp 29–45

Sears ER (1977) An induced mutant with homoeologous pairing in common wheat. Can J Genet Cytol 19:778–786

Sourdille P, Singh S, Cadalen T, Brown-Guedira GL, Gay G, Qi L, Gill BS, Dufour P, Murigneux A, Bernard M (2004) Microsatellite-based deletion bin system for the establishment of genetic–physical map relationships in wheat (*Triticum aestivum* L.). Funct Integr Genom 4:12–25

Tsujimoto H, Tsunewaki K (1988) Gametocidal genes in wheat and its relatives. III. Chromosome location and effects of two *Aegilops speltoides*-derived gametocidal genes in common wheat. Genome 30:239–244

Venske E, Santos RS, Busanello C, Gustafson P, Oliveira AC (2019) Bread wheat: a role model for plant domestication and breeding. Hereditas 156:16

Wang S, Wong D, Forrest K, Allen A, Huang BE, Maccaferri M, Salvi S, Milner SG, Cattivelli L, Mastrangelo AM, Whan A, Stephen S, Barker G, Wieseke R, Plieske J, International Wheat Genome Sequencing Consortium, Lillemo M, Mather D, Appels R, Dolferus R, Brown-Guedira G, Korol A, Akhunova AR, Feuillet C, Salse J, Morgante M, Pozniak C, Luo MC, Dvorak J, Morell M, Dubcovsky J, Ganal M, Tuberosa R, Lawley C, Mikoulitch I, Cavanagh C, Edwards KJ, Hayden M, Akhunov E (2014) Characterization of polyploid wheat genomic diversity using a high-density 90,000 single nucleotide polymorphism array. Plant Biotechnol J 12:787–796

Wang H, Sun S, Ge W, Zhao L, Hou B, Wang K, Lyu Z, Chen L, Xu S, Guo J, Li M, Su P, Li X, Wang G, Bo C, Fang X, Zhuang W, Cheng X, Wu J, Dong L, Chen W, Li W, Xiao G, Zhao J, Hao Y, Xu Y, Gao Y, Liu W, Liu Y, Yin H, Li J, Li X, Zhao Y, Wang X, Ni F, Ma X, Li A, Xu SS, Bai G, Nevo E, Gao C, Ohm H, Kong L (2020) Horizontal gene transfer of *Fhb7* from fungus underlies Fusarium head blight resistance in wheat. Science 368:eaba5435

Zhang R, Hou F, Feng Y, Zhang W, Zhang M, Chen P (2015) Characterization of a Triticum aestivum–Dasypyrum villosum T2VS 2DL translocation line expressing a longer spike and more kernels traits. Theor Appl Genet 128:2415–2425

Zhang W, Cao Y, Zhang M, Zhu X, Ren S, Long Y, Gyawali Y, Chao S, Xu S, Cai X (2017) Meiotic homoeologous recombination-based alien gene introgression in the genomics era of wheat. Crop Sci 57:1189–1198

Zhang W, Zhang M, Zhu X, Cao Y, Sun Q, Ma G, Chao S, Yan C, Xu S, Cai X (2018a) Molecular cytogenetic and genomic analyses reveal new insights into the origin of the wheat B genome. Theor Appl Genet 131:365–375

Zhang W, Zhu X, Zhang M, Chao S, Xu S, Cai X (2018b) Meiotic homoeologous recombination-based mapping of wheat chromosome 2B and its homoeologues in *Aegilops speltoides* and *Thinopyrum elongatum*. Theor Appl Genet 131:2381–2395

Zhang W, Zhu X, Zhang M, Shi G, Liu Z, Cai X (2019) Chromosome engineering-mediated introgression and molecular mapping of novel Aegilops speltoides-derived resistance genes for tan spot and Septoria nodorum blotch diseases in wheat. Theor Appl Genet 132:2605–2614

Zhang M, Zhang W, Zhu X, Sun Q, Chao S, Yan C, Xu S, Fiedler J, Cai X (2020) Partitioning and physical mapping of wheat chromosome 3B and its homoeologue 3E in *Thinopyrum elongatum* by inducing homoeologous recombination. Theor Appl Genet 133:1277–1289

Zhao R, Wang H, Xiao J, Bie T, Cheng S, Jia Q, Yuan C, Zhang R, Cao A, Chen P, Wang X (2013) Induction of 4VS chromosome recombinants using the CS *ph1b* mutant and mapping of the wheat yellow mosaic virus resistance gene from *Haynaldia villosa*. Theor Appl Genet 126:2921–2930